RELIABLE MESH MORPHING APPROACH TO HANDLE ICING SIMULATIONS ON COMPLEX MODELS

Emiliano Costa

D'Appolonia SpA, Viale Cesare Pavese 305,
Rome, 00144, Italy
emiliano.costa@dappolonia.it
http://www.dappolonia.it

Marco E. Biancolini, Corrado Groth

Università di Roma Tor Vergata, Dipartimento di Ingegneria dell'Impresa, Via del Politecnico 1,
Rome, 00133, Italy
biancolini@ing.uniroma2.it
http://dii.uniroma2.it

Giorgio Travostino, Gabriele D'Agostini

Piaggio Aerospace, Viale Generale Disegna 1,
Villanova d'Albenga,17038, Italy
gtravostino@piaggioaerospace.it
http://piaggioaerospace.it

Abstract
This paper deals with the proposal of a reliable and accurate mesh morphing based technique to efficiently handle ice accretion simulations on models of industrial interest. Such an approach is based on the mathematical framework of radial basis functions, and it can be employed together with detailed CFD analyses to dynamically mould aircraft's geometries so as to mimic the growth of ice, even when complex shapes need to be reproduced. Providing that the position of mesh nodes can be altered, the meshless characteristic of the proposed approach enables its utilization with all CFD solvers and design strategies. The main implication of the usage of radial basis is an enhanced performance and reliability in managing rough icing shapes due to, respectively, the fast application of the smoothing of volume cells and the accuracy in controlling surface mesh nodes position. To show the effectiveness of such a technique, predefined ice profiles, calculated by means of an ice accretion tool, were successfully applied on a 2d case, the NACA0012 airfoil, and on a 3d case, the HIRENASD model, using both commercial and open source CFD solvers. Those icing simulations are part of an explorative set of studies that focused on addressing the numerical strategies to be adopted in the development of the EU FP7 Project RBF4AERO.

Keywords ice accretion, mesh morphing, radial basis functions, computational fluid dynamics, meshless approach, nodes control accuracy.

1. Introduction

Flying in icing atmospheric conditions can be a serious safety problem. Ice build-up generally occurs when supercooled droplets impinge on aircraft surfaces, most commonly the engine lip and the windward face of the wings, causing a variation in the overall vehicle fluid dynamics. As ice accretions can increase the drag force and decrease the lifting characteristics of the airfoil, more power and a greater angle of attack (AoA) is required to maintain flight conditions. Moreover, wing icing causes not only stall to occur at lower attack angles, but it can diminish dangerously the vehicle maneuverability if an uneven ice distribution occurs.
In-flight icing has been responsible for more than 819 deaths and 583 plane crashes in a 19 years span period between 1982 and 2000 in the USA only. Understanding and studying the icing problem is of capital importance and an ice accretion analysis has thus become a must during the design process. Ice build-up can be investigated by means of flight tests, wind tunnels or numerical simulations. Flight tests are the most realistic and expensive means and, consequently, they are used in certain conditions only or in the final stage of the analysis. Wind tunnels can recreate exact ice shapes, but the control over the dimensionless parameters can be very hard. Computational Fluid Dynamics (CFD) is widely employed because it is a low cost alternative that can simulate with a high level of reliability and accuracy the whole icing process allowing to change a large number of parameters. Although NASA and DERA historically were the main contributors to the development of ice accretion models, including Lewice (NASA) and Trajice (DERA), nowadays there are also some other tools

coming from the major international agencies such as Capta (ONERA), Multi-ice (CIRA) and FENSAP-ICE (NTI).
With regard to the RBF4AERO Project, whose objectives are briefly specified in the following section, two methodological approaches are envisaged to be put in practice. According to the first one, termed frozen or constrained, icing simulations are carried out by imposing, at specific iterations of the CFD computing, the icing profiles calculated by means of an icing accretion tool at predefined instants of time. The second one, referred to as "on the fly" or evolutionary, foresees the use of an accretion code that, in conjunction with a CFD solver, modifies dynamically the numerical grid according to the calculated ice accretion.
The frozen approach allows to estimate the ability of mesh updating tools, usually founded on remeshing and/or adaption but on RBF mesh morphing in this study, to manage complex ice shapes. Moreover it can be used even in cases in which a detailed local accretion model is not available and ice shapes are known from experiments, from a literature database or are interpolated using simplified models (for instance a complex 3d shape can be approximated using 2d accretion tools in a certain number of cross sections).
In the present work we present the results obtained with the frozen approach and they are described hereinafter.

2. Background of RBF Mesh Morphing Applied to CAE

Radial Basis Functions (RBFs) are a class of mathematical interpolation functions that, in Computer Aided Engineering (CAE) applications, can be used to drive the morphing (smoothing) of the computational model discretized domain by applying predefined displacements to a set of purposely generated points, called source points.
The main characteristics of such an approach are the meshless property, the preservation of mesh consistency and the low disk usage in addition to standard calculation, whilst some among its main advantages are the exact control of nodes during smoothing, the prevention of remeshing noise, the possibility to be fully integrated in the computing process and the high performance in handling large models.
The RBF mesh morphing technique is the major technology of the RBF4AERO Project (European Commission, 2013) which has the purpose to develop the RBF4AERO Benchmark Technology, namely an integrated numerical platform and methodology to efficiently face the most demanding challenges of aircrafts design and optimization. This project is a great opportunity to further boost and extend the application of mesh morphing in the aviation sector after it received lots of acknowledgments in other industrial fields such as automotive (Sovani and Khondge, 2012), motorsport (Caridi and Wade, 2012; Petrone and Biancolini, 2014), naval (Biancolini *et al.*, 2014) and medical (Biancolini *et al.*, 2012). In particular, the intent of RBF4AERO is to cover modern aeronautical design applications such as shape optimization (Biancolini *et al.*, 2013), ice accretion simulation (Biancolini and Groth, 2014), fluid-structure interaction (FSI)(Cella and Biancolini, 2012; Reina *et al.*, 2014), adjoint-morphing coupling and multi-physics optimization analyses through efficient procedures based on RBF mesh morphing, such to prevent the typical compromise of standard optimization procedures in terms of speed, accuracy and extent, and thus to relevantly reduce design process duration.

3. Methodological Strategy of the Frozen Approach

RBFs are an efficient numerical means to control the computational grid in icing applications, thanks to its exact local control capability. By exploiting such a feature, in accordance with the frozen approach it is possible, instead of being forced to regenerate the mesh following the evolution of ice profiles, to quickly apply the new shape of ice by imposing, to each surface node, its corresponding displacement previously evaluated by means of an ice accretion model (icing data). Such an operation is performed at specific iterations of CFD computing, steady or unsteady depending on the assumption of the analysis, acting on the source points extracted from surface mesh. In that manner, the geometry actually covered by ice is suitably moulded and the surrounding cells' nodes are accordingly adjusted by volume mesh smoothing. The workflow of the proposed RBF mesh morphing based approach is visualized in Figure 1 through a block diagram.

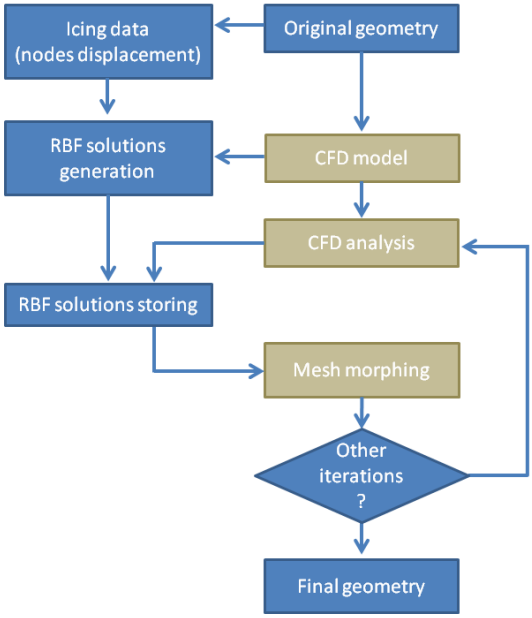

Fig. 1. Workflow of the frozen approach for ice accretion simulation.

Such a workflow, carried out utilizing OpenFOAM® (release 2.3.0), Metacomp Technologies CFD++® and ANSYS® Fluent® for the CFD computing and RBF Morph™ for the morphing task, foresees the accomplishment of two subsequent stages. In the first one, 2d or 3d ice profiles are evaluated for each step of icing through an ice accretion tool and, then, exported according to a predefined format in which the coordinates and displacement components for each point of the accreted surface are specified. Those data, referred to as icing data, constitutes the input for the generation of RBF solutions that are finally saved for successive use. The second stage deals with the icing simulation in which a certain number of CFD iterations are performed and the stored RBF solutions are properly applied to update the grid of the computational model.
It is worth to underline that, in the most efficient computational scenario that will be controlled by the RBF4AERO Benchmark Technology when completely developed, the original (baseline) mesh is used only for computing since the morpher tool accomplishes the task of the modification of parameters and geometry through mesh update.

4. Icing Profiles and RBF Solutions Set-Up

4.1. *2d case - NACA0012*

The geometry selected to develop the 2d study is the NACA0012 airfoil. The flow conditions imposed for running CFD analyses are Mach=0.5, Re=$11.56 \cdot 10^6$ and 4650 ft (1417.12 m). Adopting the afore-reported conditions, the ice growth was evaluated through an ice accretion tool implemented in CFD++ till 21 minutes for three values of AoA, namely 0, 2 and 4 degrees, using a Langmuir-D distribution and setting Delta Isa equal to -25° and the median volume diameter (MVD) to 20 μm.
Relating to icing steps, it was decided to save the icing profiles at 7, 14 and 21 minutes (frozen profiles) in view of defining the icing data required by the morpher tool to apply surface mesh smoothing according to what was earlier described.
The gained results are illustrated in Figure 2. Specifically the 2d profiles for the AoA equal to 0, 2 and 4 degrees are respectively plotted from left to right. In each image, the baseline profile of NACA0012 airfoil in proximity of the leading edge as well as the frozen profiles are plotted. In the lift configurations the effect of the AoA on ice accretion is well visible.

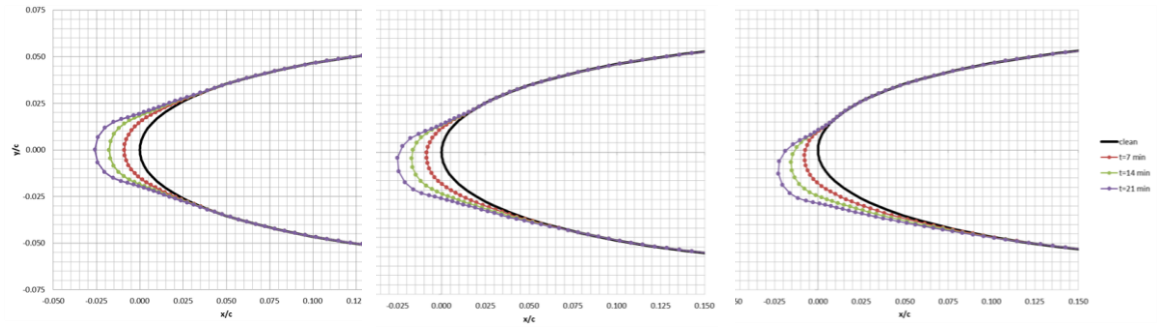

AoA=0° **AoA=2°** **AoA=4°**

Fig. 2. Ice profiles calculated for NACA0012 airfoil.

In order to verify the proposed method we have decided to compare a standard reference workflow, developed through CFD++ computing, in which a new mesh is generated for each shape with the new one, developed through OpenFOAM, in which the proposed mesh morphing approach is employed.
The standard reference workflow foresees the generation of twelve meshes to run the CFD studies using the CFD++ solver. Referring to this latter, Figure 3 depicts the 2d structural quadrangular grid (left) and a detail of it near the NACA0012 airfoil (right) for the baseline no-lift configuration.

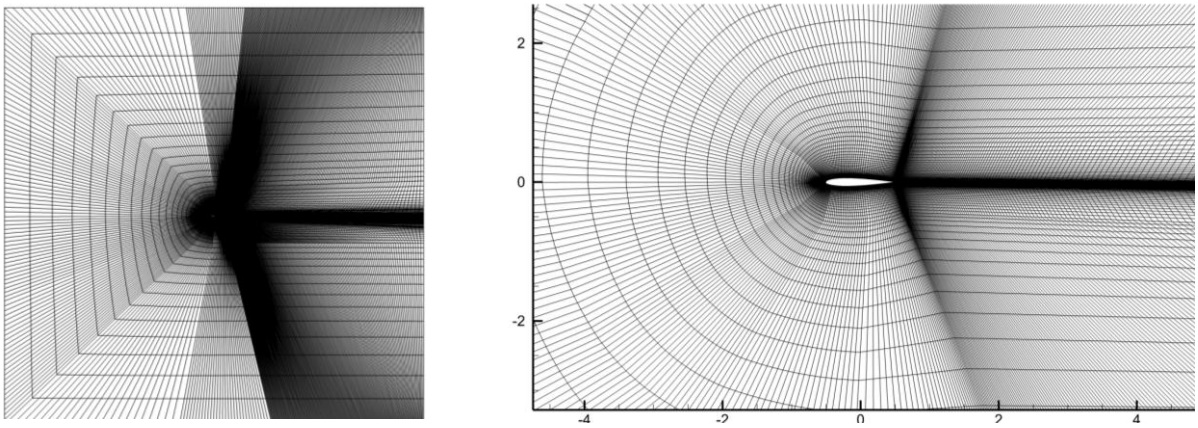

Fig. 3. Mesh of the NACA0012 case to be run through CFD++ (baseline for AoA=0°).

A detail of NACA0012 profile in the CFD++ meshes at AoA=4° respectively for 7, 14 and 21 minutes is depicted in Figure 4.

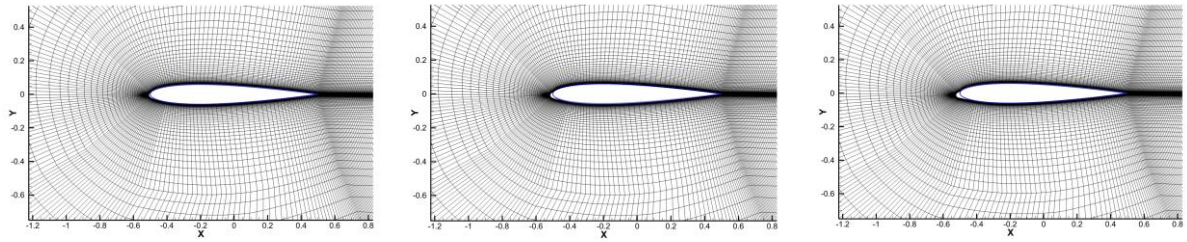

Fig. 4. Mesh of the NACA0012 case to run ice profiles configurations for AoA=4° through CFD++.

To perform the 2d simulations using OpenFOAM, a 3d hexahedral structured mesh is required. Given that, cells were created extruding a single layer of hexahedron starting from a 2d mesh composed by 9.8 $\cdot 10^3$ quadrilateral faces. Figure 5 illustrates the computational domain (left), extended around 20 wing chords upstream the model, 25 downstream and 30 on the top and bottom, and a detail of the extrusion of the discretized NACA0012 airfoil (right). The shape of the domain was designed to allow the use of the same grid for all AoAs.

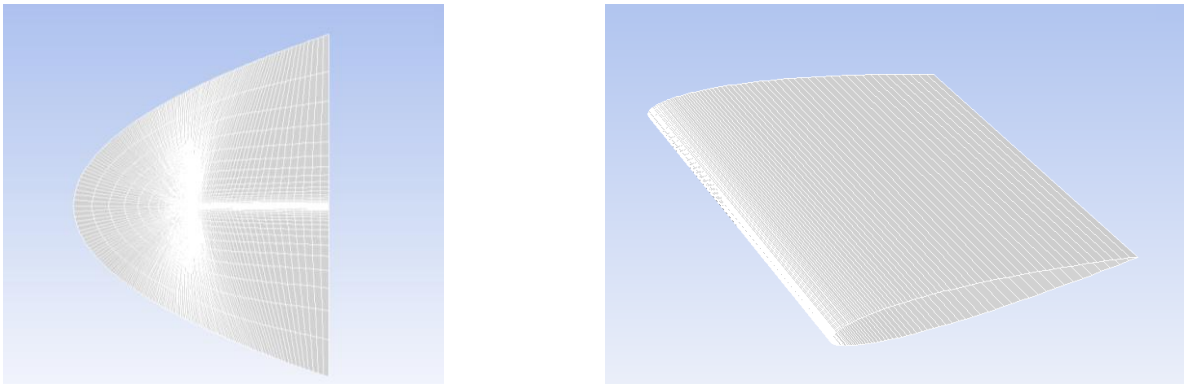

Fig. 5. Mesh of the NACA0012 case to be run through OpenFOAM.

The RBF solutions were generated adopting the two-step procedure of the morpher tool (RBF Morph, 2014a). According to such a strategy, in the first step the RBF solution involving just the surface nodes displacements is generated, whilst in the second step the solution of the first step is loaded and imposed as constraint for surface mesh displacement. The same structure of such a RBF set-up was used for all icing configurations.
Considering what just described, the whole RBF set-up reflects this resolution choice. In fact, in the first RBF solution (first-step) the NACA0012 profile is deformed by assigning the icing data only at the wing surface nodes using the Points feature of the morpher (RBF Morph, 2014b). Figure 6 depicts the preview of the source points position before (left) and after morphing for the case with AoA=4° at 7 minutes.

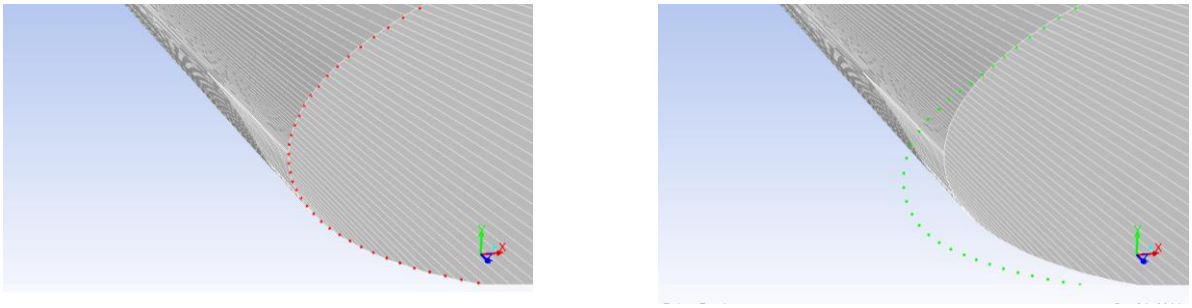

Fig. 6. Source points before (left) and after (right) morphing for the case AoA=4° at 7 minutes.

In the RBF set-up of the second step the first one is assigned to airfoil mesh. To complete the set-up, a box-shaped domain encap was added to delimit the action of morphing in the computational domain (source points at surface boundaries have null displacement by definition). The source points distribution in the domain encap is depicted in Figure 7.

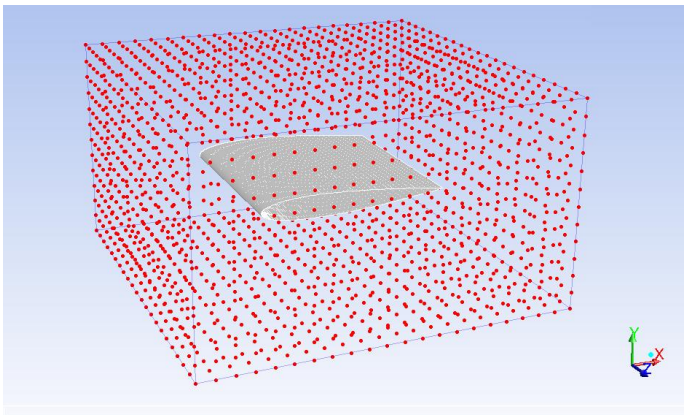

Fig. 7. Source points of the box-shaped domain encap for the NACA0012 case.

To highlight the effect of RBF solutions on the airfoil mesh, Figure 8 illustrates a preview of the shape of the baseline configuration overlapped to the morphed ones for the considered AoAs.

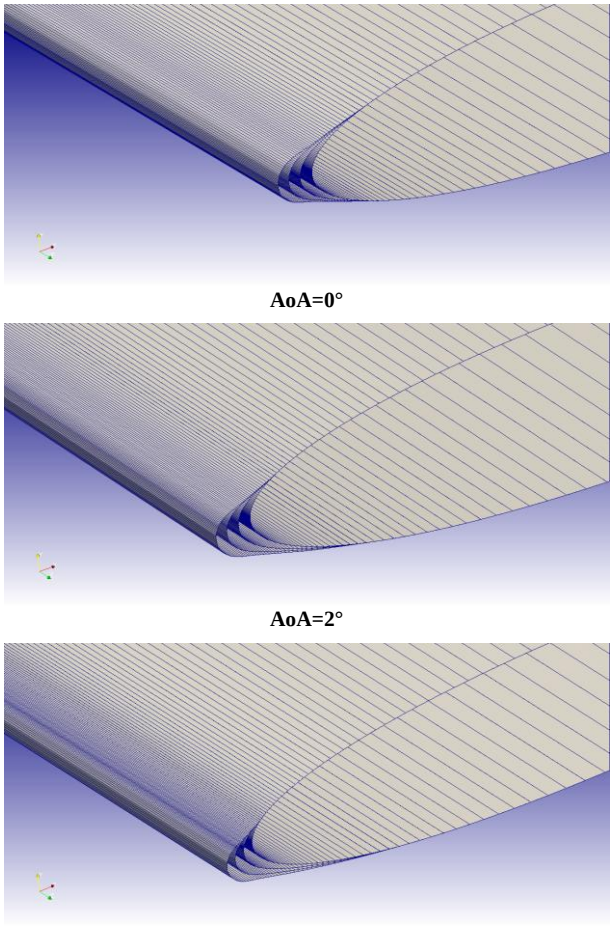

Fig. 8. Preview of the effect of RBF solutions for the three AoAs.

Once created, all those solutions are available and can be called during OpenFOAM computing to gain what is described in the following section of computational results.

4.2. *3d case - HIRENASD*

The 3d model used to show how the proposed technique is capable to succeed also with the real world aircraft icing applications, is one of the configurations supplied to participate to the Aeroelastic Prediction Workshop (AePW) launched with the main purpose to assess the capability of the most advanced numerical methods in predicting static and dynamic aeroelastic phenomena and responses (Heeg *et al.*, 2013). In particular, the test case of interest, referred to as HIgh REynolds Number Aero-Structural Dynamics (HIRENASD), is shown in Figure 9. It consists of a tapered 34° aft-swept wing with a BAC3-11/RES/30/21 supercritical airfoil profile, having a chord of 0.3445 m, that was tested in the Cologne European Transonic Wind tunnel (ETW).

Fig. 9. HIRENASD wind tunnel model.

The volume mesh and a detail of the surface mesh of the HIRENASD model are shown in Figure 10 on the left and right side respectively. Exploiting the symmetry of the flow field, the mesh models just half domain. That grid is a multi-block structured hexahedral, it is extended around 40 wing chords upstream the model, 42 downstream and 43 on the side, and since it was created satisfying industrial standards, it is aggressive low-Re with wall cells clustering aimed to solve the boundary layer up to the wall.

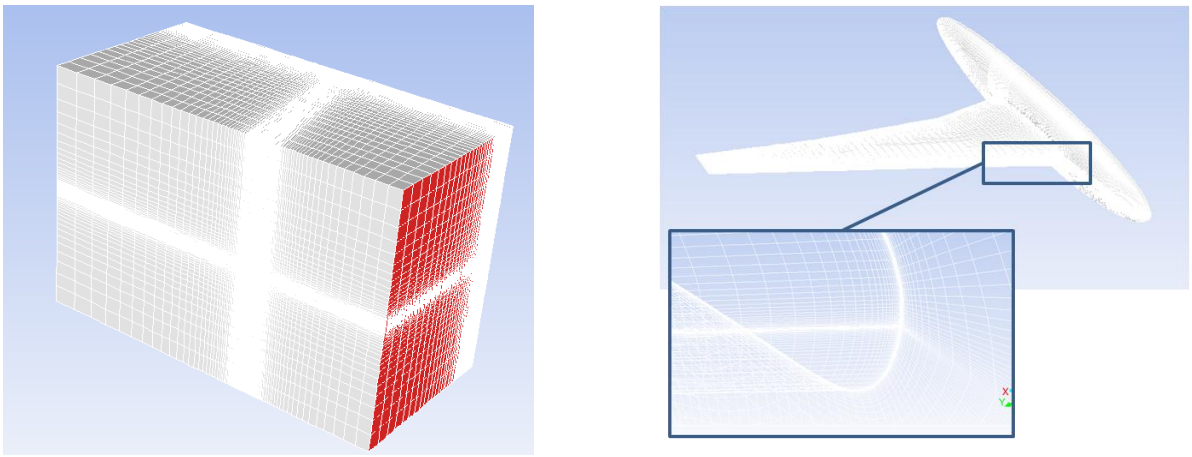

Fig. 10. Mesh of the HIRENASD case.

To generate the RBF solutions for the HIRENASD model, the same strategy employed for NACA0012 was adopted. Figure 11 reports the position of the source points before (left) and after morphing for the first-step solution corresponding to 7 minutes of ice accretion. Specifically, the nodes of the wing in the area that are not covered by ice have a null displacement, whereas for the remaining ones the displacement is dictated by icing data.

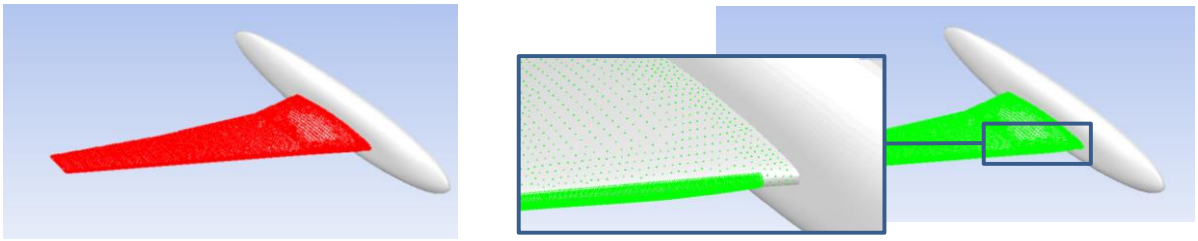

Fig. 11. Distribution of the source nodes before and after morphing for 7 minutes solution for the HIRENASD case.

The source points distribution in the cylinder-shaped domain encap used for the second-step solution, wrapping the leading edge of the HIRENASD model, is depicted in Figure 12.

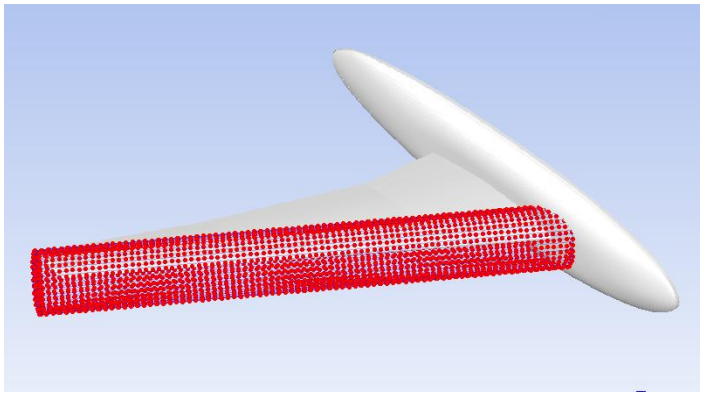

Fig. 12. Preview of the source points of the cylinder-shaped domain encap for the HIRENASD case.

In the following sections the CFD set-up and results for both the studied cases are respectively detailed.

5. CFD Set-up and Results

5.1. *2d case - NACA0012*

The principal parameters and models used to perform the twelve simulations of the standard workflow by means of CFD++ are summarized in Table I. In this case the employed solver provides a steady solution.

Table I. Main parameters and models used for CFD++ runs.

Parameter / Model	Type	Value
Solver	Compressible PG navier-Stokes/euler	-
Turbulence model	Spalart-Allmaras	-
Nu_tilda	-	$1.09 \cdot 10^{-4}$ $m^2 \cdot s^{-1}$
Freestream turbulence level	-	0.002
Turbulent/laminar viscosity ratio	-	50
Farfield (boundary condition)	Inflow/Outflow Characteristics-based	-

The proposed mesh morphing approach takes into account the interval of time between an icing step and the subsequent one (7 minutes) to compute the fully developed flow solution for each AoA. In this case ice evolution required four sequential simulations that were performed for each AoA controlling OpenFOAM by means of a batch file. The principal parameters and models used to run simulations are summarized in Table II. Since rhoPimpleFoam is a transient solver and the morphing action allows to maintain unaltered the mesh topology, a total time of simulation of 0.5 s was covered for each icing step and the final solution was used as a starting point for the subsequent analysis.

Table II. Main parameters and models used for OpenFOAM runs.

Parameter / Model	Type	Value
Solver	rhoPimpleFoam	-
Turbulence model	Spalart-Allmaras	-
Inlet boundary condition	Velocity inlet	-
Outlet boundary condition	Fixed pressure with zero gradient	-
Time step	-	$1.0 \cdot 10^{-7}$
Time step management	Adaptive	-
Courant	Maximum value	5

In Figure 13, Figure 14 and Figure 15 the comparison between the coefficient of pressure computed by OpenFOAM and CFD++ at 7, 14 and 21 minutes for the AoA equal to 0, 2 and 4° are respectively reported.

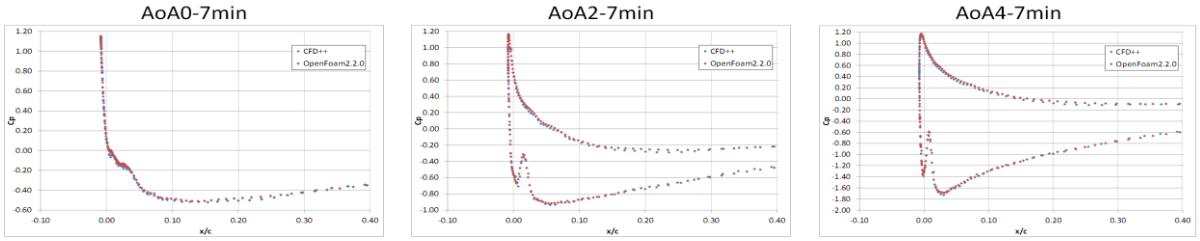

Fig. 13. Comparison of coefficient pressure profiles computed in the NACA0012 case at 7 minutes.

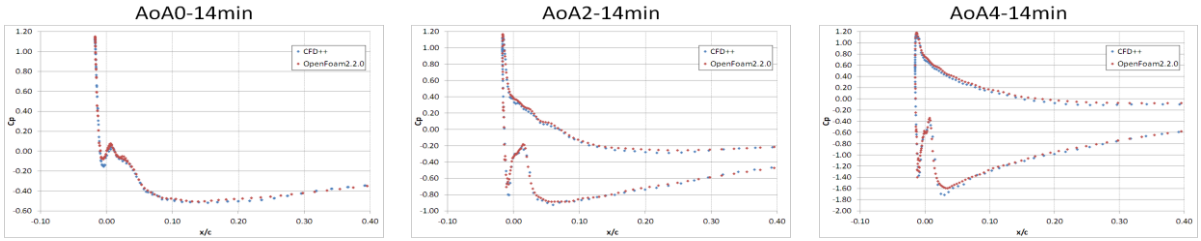

Fig. 14. Comparison of coefficient pressure profiles computed in the NACA0012 case at 14 minutes.

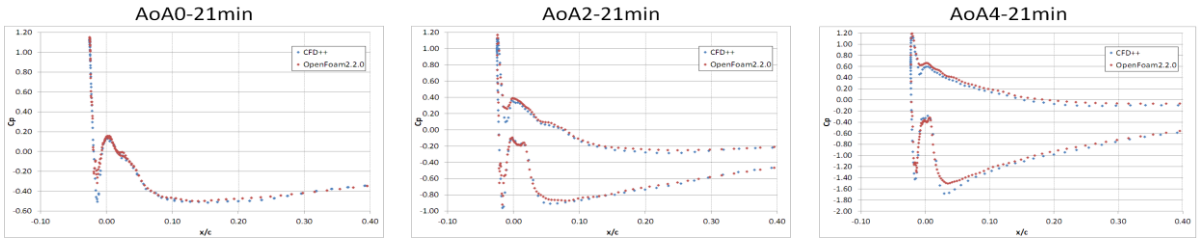

Fig. 15. Comparison of coefficient pressure profiles computed in the NACA0012 case at 21 minutes.

As visible, the outputs compare favorably well. This achievement gives the evidence that the morphing action is effective and accurate in the reproduction of icing profiles. Given that, the time that the proposed approach allows to save can be straightforwardly understood and quantified by users.

5.2. *3d case - HIRENASD*

In the case of HIRENASD, the numerical analyses in steady conditions were run in sequence by means of Fluent using a journal file. The main parameters and models used to run simulations are reported in Table III.

Table III. Main parameters and models used for Fluent runs.

Parameter / Model	Type	Value
Solver	Density based	-
Solver type	Implicit	-
Turbulence model	k-ω SST	-
Air	Ideal gas	-
Farfield boundary condition	Inflow/Outflow characteristics-based	-
Courant	Maximum value	4

Figure 16 shows, from top left to bottom right, the relative pressure distribution on the HIRENASD model for the fully developed flow in steady conditions respectively for the baseline (a), 7 (b), 14 (c) and 21 (d) minutes configuration. In those images the monitoring sections, that are the sections of the wing at which the pressure coefficient profiles were monitored during computing, are also visible. In particular, those sections respectively correspond to 15.7% (Section 1), 40.8% (Section 2) and 73.1% (Section 3) of the wing span equal to 1.548 m.

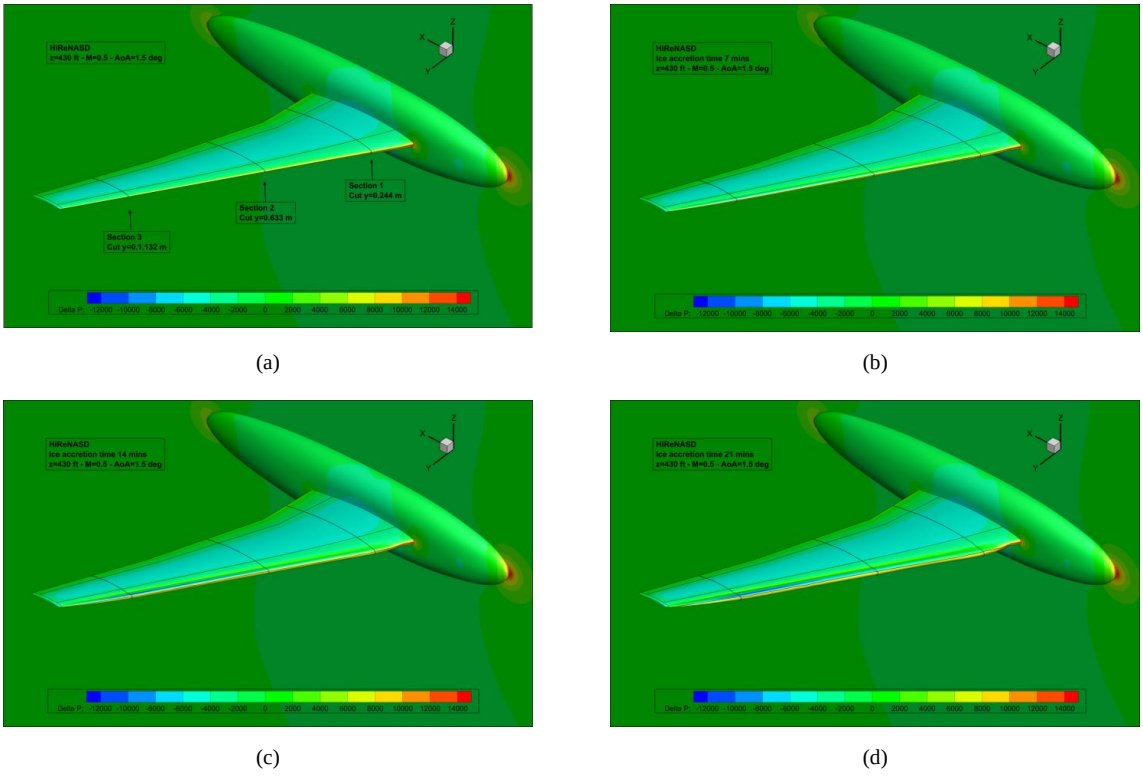

Fig. 16. Relative pressure distribution in steady conditions for all configurations.

Figure 17 depicts, for the baseline configuration, the wing section profile (continuous line) and the coefficient of pressure (the dotted line) along Section 1, Section 2 and Section 3 going from left to right respectively.

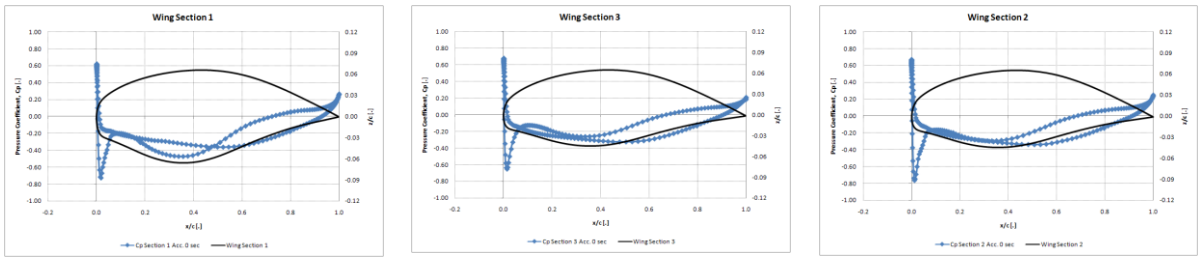

Fig. 17. Wing section profile and the coefficient of pressure for the baseline configuration.

Figure 18, Figure 19 and Figure 20 illustrate, respectively at 7, 14 and 21 minutes, the same results reported in Figure 17. Going on in time at the icing growth significantly changes the leading edge of each section and so the effective profile induces a relevant variation of the distribution of the pressure coefficient. Such a contribution must be accounted to suitably predict the unwanted effects on aircraft maneuverability and to design the deicing system.

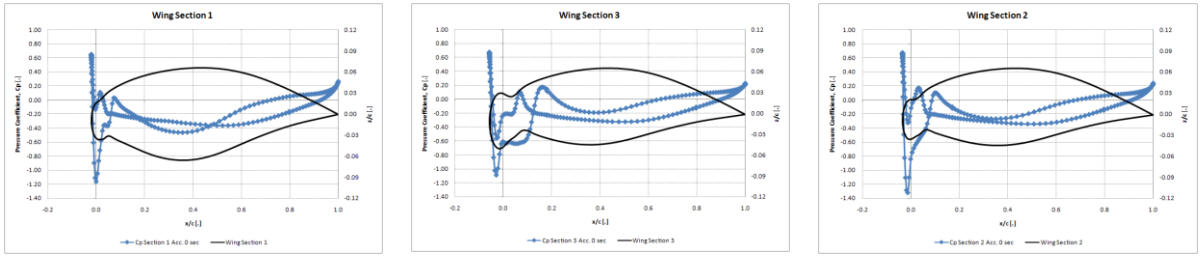

Fig. 18. Wing section profile and the coefficient of pressure for the configuration at 7 minutes.

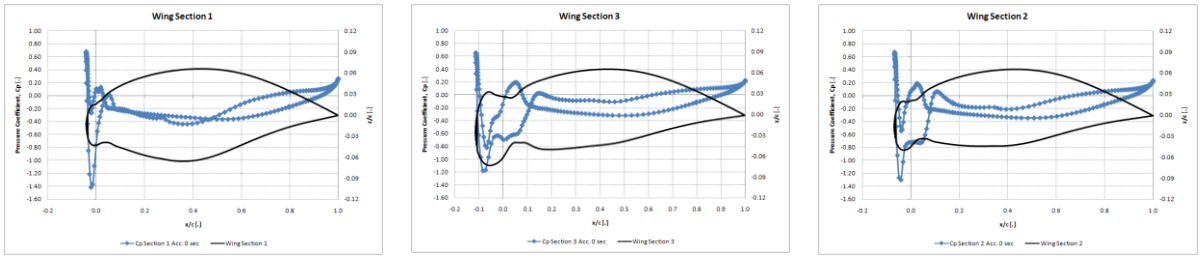

Fig. 19. Wing section profile and the coefficient of pressure for the configuration at 14 minutes

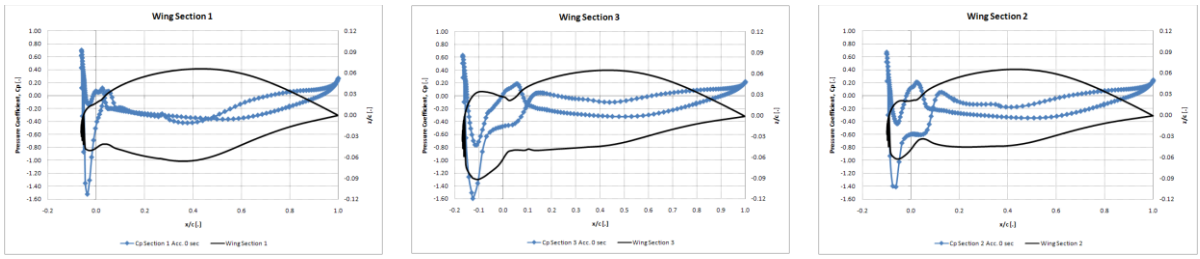

Fig. 19. Wing section profile and the coefficient of pressure for the configuration at 21 minutes.

The latter image particularly evidences how the proposed approach is capable to reliably manage rough and challenging ice surfaces because the ice accretion reaches about the 15% of the wing chord.

6. Concluding Remarks

In this paper a mesh morphing technique to effectively manage ice accretion simulations through CFD was described. The morphing is founded on the class of mathematical interpolation function RBFs, allowing to control very fast and in exact manner the smoothing of surface mesh nodes for the virtual reproduction of icing profiles. To demonstrate the reliability of the proposed approach, the ice growth on 2d and 3d models was carried out according to the frozen strategy, envisaging the imposition of predefined ice profiles previously determined by means of an ice accretion tool.

The study performed in the 2d case demonstrated the accuracy of the approach that compares very well with a standard workflow based on generation from scratch, whilst the 3d case mainly evidenced the reliability of its use due to the high challenging peculiarity of the reproduced ice profiles.

The proposed method results to be quite general, in the sense that it can be employed in all optimization procedures and CFD solvers on condition that the position of mesh nodes is modifiable. However, to gain satisfactory and accurate results for the icing applications, the mesh of the computational model is required to be structured and of high quality. Relating to CFD solution stability, it basically depends on the CFD solver robustness because morphing typically introduces a degradation of the mesh quality.

Considering what gained, the mesh morphing strategy, object of the present work, is a good candidate to also handle the “on the fly” approach.

As a closing consideration on the social impacts, in the sectors in which the ice accretion study is relevant, such as for aircrafts design and wind turbine design and optimization, a general increasing of safety for people is expected.

Acknowledgments

This work was financially supported by the RBF4AERO project funded in part by the EUs 7th Framework Programme (FP7-AAT, 2007 - 2013) under Grant Agreement no. 605396.

References

Cella, U. and Biancolini, M. E. (2012). Aeroelastic Analysis of Aircraft Wind-Tunnel Model Coupling Structural and Fluid Dynamic Codes. *Journal of Aircraft*, Vol. 49, No. 2 (2012), pp. 407-414.

Biancolini, M.E., Ponzini, R., Antiga, L. and Morbiducci, U. (2012). A new workflow for patient specific image-based hemodynamics: parametric study of the carotid bifurcation. *Summer School held by CILEA - Conference CompIMAGE 2012*.

Biancolini, M.E., Travostino, G. and Mancini, M. (2013). Shaping up – Mesh morphing reduces the time required to optimize an aircraft wing. *ANSYS Advantage Magazine - Volume VII, Issue 1*.

Biancolini, M.E., Viola, I.M. and M. Riotte (2014). Sails trim optimisation using CFD and RBF mesh morphing. *Computers and Fluids*, Elsevier, Volume 93, 10 April 2014, Pages 46–60. DOI: 10.1016/j.compfluid.2014.01.007.

Biancolini, M.E. and Groth, C. (2014). An Efficient Approach to Simulating Ice Accretion on 2D and 3D Airfoils. *Advanced Aero Concepts, Design and Operations, 2014*.

Caridi, D. and Wade, A. (2012). Higher-Speed CFD. *Professional Motorsport World Magazine*.

European Commission (2013). RBF4AERO Project - "Innovative benchmark technology for aircraft engineering design and efficient design phase optimisation".

Heeg, J., Chwalowski, P., Florance, J.P., Wieseman, C.D., Schuster, D.M. and Perry III, B. (2013). Overview of the Aeroelastic Prediction Workshop. *American Institute of Aeronautics and Astronautics*.

Petrone, G., Hill, C. and Biancolini, M.E (2014). Track by Track Robust Optimization of a F1 Front Wing using Adjoint Solutions and Radial Basis Functions. *44th AIAA Fluid Dynamics Conference*, AIAA-2014-3174.

RBF Morph (2014). RBF Morph – Best Practices Guide.

RBF Morph (2014). RBF Morph - Users Guide.

Reina, G.P., Della Sala, A., Biancolini, M.E., Groth, G. and Caridi D. (2014). Store Separation: Theoretical Investigation of Wing Aeroelastic Response. *4th Aircraft Structural Design Conference*.

Sovani, S. and Khondge, A. (2012). Scaling New Heights in Aerodynamics Optimization: The 50:50:50 Method. *White paper available on ANSYS Inc. Website*.

Acronyms and Abbreviations Used

AAT	Aeronautics and Air Transport
AePW	Aeroelastic Prediction Workshop
AoA	Angle of Attack
CAE	Computer-Aided Engineering
CFD	Computational Fluid Dynamics
CFD++	CFD++®
ETW	European Transonic Wind (tunnel)
EU	European Union
Fluent	ANSYS® Fluent®
FP7	Seventh Framework Programme
FSI	Fluid-Structure Interaction
HIRENASD	HIgh REynolds Number Aero-Structural Dynamics
MVD	Median Volume Diameter
OpenFOAM	OpenFOAM®
RBF(s)	Radial Basis Function(s)
RBF Morph	RBF Morph™